WEP Warwick Evans Publishing

International Journal of Materials Science and Technology Studies

ISSN: 3006-7693 (Print), ISSN: 3006-3744 (Online) | Volume 3, Number 2, Year 2025
DOI: https://doi.org/10.62051/ijmsts.v3n2.08
Journal homepage: https://wepub.org/index.php/IJMSTS/index

Research Progress on X-site Doping of All-inorganic Perovskite CsPbX3 Nanocrystals

Xuanrui Xiang, Hanyue Guan, Liting Zhao, Huiping Lu *

School of Tiangong University, Tianjin 300387, China
*Corresponding Author: Huiping Lu

ABSTRACT

All-inorganic perovskite $CsPbX_3$ (X=Cl, Br, I) nanocrystals have attracted extensive attention due to their excellent photoelectric properties. These materials not only have the advantages of tunable emission wavelength, emission peak width and high fluorescence quantum yield, but also are significantly superior to traditional organic-inorganic hybrid systems in terms of device compatibility and environmental stability. They have shown great application potential in the field of optoelectronic devices and have been successfully applied to the construction of functional modules such as light-emitting layer (LEDs), photovoltaic light-absorbing layers and laser gain medium. In recent years, it has become a research hotspot to regulate the physical and chemical properties of $CsPbX_3$ nanocrystals through ion doping engineering. The doping strategy can effectively adjust the band structure and luminescence properties of the material, and its mechanism is mainly due to the perturbation of the crystal field and the modification of the defect state by the doping elements. In this paper, the international research trends of X-site doping of this material are systematically reviewed. The crystal structure characteristics, optical performance regulation mechanism and mainstream preparation technology are described. The optimization mechanism of halogen site chemical modification on the photoelectric properties of materials is analyzed. Finally, the current technical bottleneck and future development direction are discussed.

KEYWORDS

Perovskite; $CsPbX_3$ nanocrystals; Doping

1. INTRODUCTION

Since the 21st century, with the vigorous development of the nano-industry, lead halide perovskite nanocrystals (PNCs) have received extensive attention due to their low cost, narrow emission peak half-width, high luminous efficiency, adjustable spectrum, and high stability. It has been successfully applied to many fields such as light-emitting diodes, solar cells, lasers, and photodetectors [1-5]. The chemical composition of $CsPbX_3$ nanocrystals follows the ABX_3-type perovskite structure with an element molar ratio of 1:1:3. In this crystal structure, the A site is occupied by monovalent cesium ions (Cs^+), the B site is composed of divalent lead ions (Pb^{2+}) as the core metal sites, and the X site is filled with halogen anions (Cl^-, Br^-, I^- or their mixed system). As shown in Fig. 1, each second-order cation is coordinated with six halogen ions through octahedral coordination to form a structural unit, while cation A is embedded in a cubic octahedral gap composed of adjacent BX_6 octahedral frameworks [6-9]. It is worth noting that the photoluminescence (PL) spectral characteristics of such nanocrystals are directly related to the type and proportion of X-site halogens. By adjusting the halogen composition, the emission wavelength can be continuously controlled in the visible range [10].

Protesescu's research team successfully prepared $CsPbX_3$ nanocrystals with adjustable starting light wavelength by adjusting the ratio of halogen precursors. This series of materials have excellent optical properties. The photoluminescence quantum yield (PLQY) can reach 50 % ~ 90 %, the half-peak width is maintained in the range of 12 - 42 nm, and the fluorescence lifetime is adjustable from 1 - 29 ns (Fig. 2 (d)) [11]. Fig. 2 (a) intuitively shows the gradual change of luminescence color of nanocrystalline toluene solutions with different halogen compositions under ultraviolet excitation, and the corresponding photoluminescence spectrum (Fig. 2 (b)) and absorption spectrum (Fig. 2 (c)) confirm the regulation of halogen components on optical properties. Compared with organic-inorganic hybrid systems, these all-inorganic nanocrystals can achieve stable exciton radiation and photoelectric response characteristics at room temperature due to their stronger exciton binding energy [12]. In order to improve the performance of materials, researchers have developed strategies such as surface ligand modification, ion doping, and lead-halogen stoichiometry optimization. Among them, precise regulation of the type and proportion of X-site halogens is one of the key ways to optimize the luminescence performance.

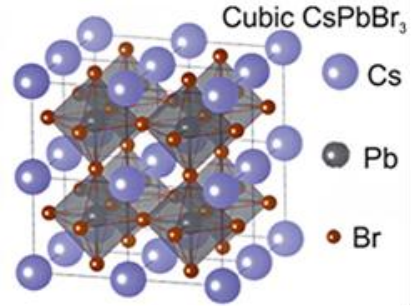

Figure 1. Perovskite structure diagram [11].

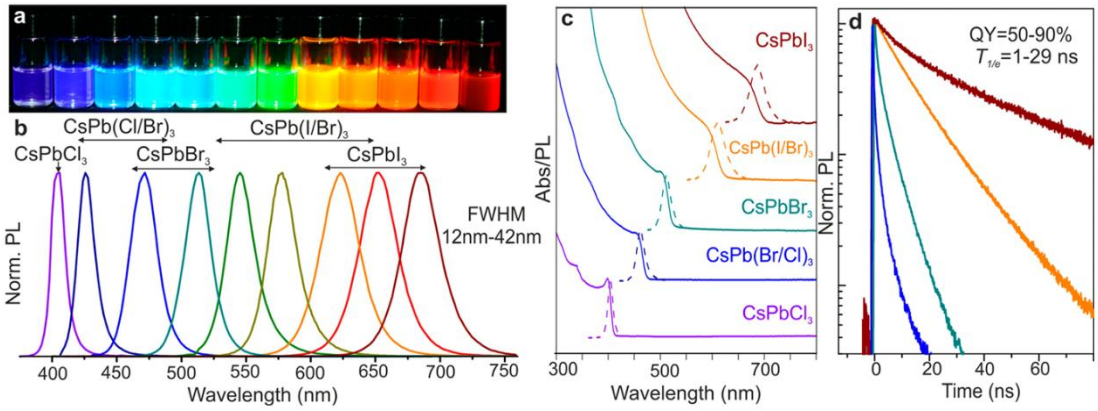

Figure 2. Luminescence properties of all-inorganic perovskite [11]: (a) All-inorganic perovskite toluene solution sample diagram of different halogens under violet light irradiation; (b) PL spectra of perovskite doped with different halogen ions; (c) Absorption spectra of different halogen perovskites; (d) Time-resolved spectra of different halogen perovskites.

In this paper, based on the basic physical and chemical properties of PNCs, various existing preparation methods are introduced. At the same time, the research progress of various improvements in the composition of halides at X-sites is described. Finally, the future development of the material is discussed in this paper.

2. PREPARATION METHOD

The main synthesis methods of $CsPbX_3$ nanocrystals include hot injection method, anion exchange method, solvothermal method, supersaturated recrystallization method, ultrasonic assisted method and microwave assisted synthesis method. As early as 1958, MLLER has reported the crystal structure of $CsPbX_3$. However, the radius of Cs ions is too small to support the perovskite framework, which is not stable at room temperature [13], limiting the development of this material. It was not until 2015 that Protesescu's group creatively used the hot injection method to synthesize a stable cubic phase $CsPbX_3$ nanocrystal structure of 4 ~ 15 nm at high temperature (140 ~ 200 °C) for the first time [11]. As shown in Fig. 3(a), the PLQY range of the cubic phase $CsPbX_3$ nanocrystals is 50 % ~ 90 %, and the half-peak width of the emission peak is 12 ~ 42 nm, which provides an important direction for the development of perovskite.

In the same year, G. Nedelcu et al. proposed the preparation of inorganic halide quantum dots with different halogens by anion exchange method [14]. By mixing different proportions of $CsPbBr_3$, $CsPbCl_3$ and $CsPbI_3$ nanocrystals, rapid anion exchange occurs between nanocrystals, as shown in Fig. 3(a). Finally, uniform CsPb $(CI/Br)_3$ and CsPb $(Br/I)_3$ nanocrystals were obtained. This method can achieve X-site doping, but the mixing of different halogens will lead to phase separation of quantum dots and affect their photostability.

The solvothermal synthesis route was innovatively proposed by Zhang Qiao's team in 2019 [15]. The specific process is to uniformly mix cesium acetate, PbX_2 and organic ligands in a high-pressure reactor (as shown in Fig. 3(c)), and then place them in a drum oven for high-temperature reaction at 160 ℃ Finally, $CsPbX_3$ nanocrystals with uniform morphology were obtained by centrifugation and purification. The materials prepared by this method not only exhibit a typical cubic crystal structure, but also exhibit excellent monodispersity.

The supersaturated recrystallization technique enables the directional interphase migration of Cs^+, Pb^{2+} and X-ions in a few seconds by regulating the distribution balance of solutes in soluble and insoluble solvents [16]. This preparation strategy has received extensive attention due to its operational advantages. In 2019, Gao Chunhong's team successfully used this method to construct a $CsPbX_3$ nanocrystalline system. By integrating the electron transport layer and the phosphorescent sensitizer, the problems of insufficient surface coverage of perovskite films, limited exciton utilization efficiency and unbalanced carrier transport were effectively improved, and finally a high-performance green light-emitting diode was developed [17].

Ultrasonically assisted synthesis is a technique based on the action of physical field. This method acts on the ternary mixed system of precursor salt, capping ligand and non-polar solvent by ultrasonic energy field to promote the in-situ formation of oleic acid-cesium complex. The composite not only has non-polar dissolution characteristics, but also can coordinate with PbX_2 to form stable $CsPbX_3$ nanocrystals [18].

Microwave synthesis technology has the advantages of high synthesis efficiency, low energy consumption and short reaction cycle. In the preparation of $CsPbX_3$ nanocrystals, the precursor raw materials need to be homogeneously mixed with oleic acid, oleylamine and 1-ODE solvent in a special quartz container. Subsequently, the reaction vessel was transferred to a microwave synthesizer, and the reaction system was accurately heated to 160 °C at a heating rate of 28 °C/min through a programmed temperature control system, and the crystallization process was completed at this temperature for 5 minutes. After natural cooling of the system, the target product can be obtained by washing and purifying with hexane [19].

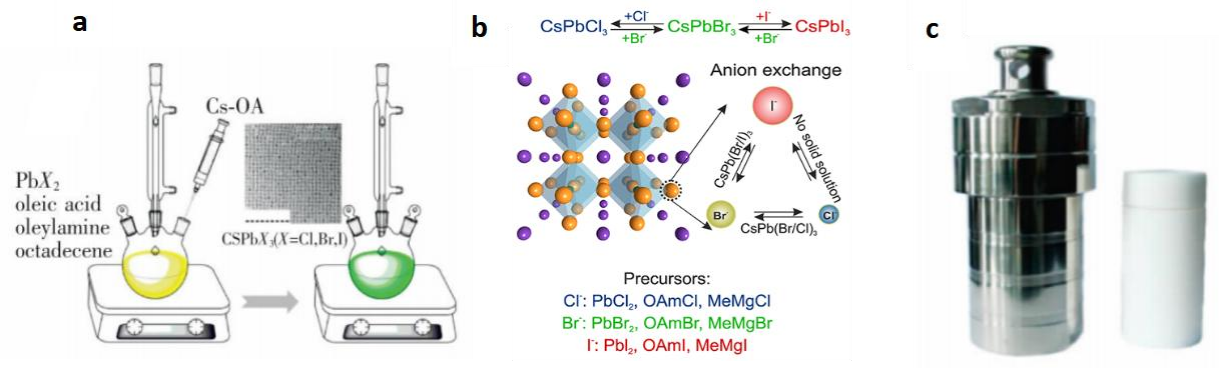

Figure 3. Thermal injection method (a) [11]; anion exchange diagram (b) [14]; solvothermal synthesis method (c) [15]错误!未找到引用源。.

3. PHYSICOCHEMICAL PROPERTIES OF CSPBX$_3$ NANOCRYSTALS

3.1. Optical Properties of CsPbX$_3$ Nanocrystals

The luminescence mechanism of $CsPbX_3$ nanocrystals follows the basic physical laws of semiconductor quantum dots. As shown in Fig. 4, under the excitation of external energy, electrons transition from the valence band to the conduction band and form electron-hole pairs. The composite luminescence process mainly includes three paths [20]: (1) direct recombination of conduction band electrons and valence band holes; (2) Radiation transition occurs after electrons are trapped by lattice defect states; (3) Electrons relax luminescence through doped ion energy levels [21].

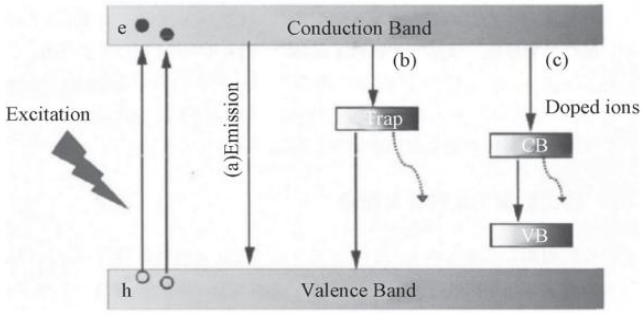

Figure 4. The schematic diagram of the luminescence principle of quantum dots [20].

The luminescence properties of the material can be precisely controlled by two strategies: the first is the size effect regulation. The decrease of the size of $CsPbX_3$ nanocrystals will cause the quantum confinement effect, resulting in the broadening of the band gap and the blue shift of the luminescence peak in the visible light region of 410 - 700 nm [22-25]. In addition, $CsPbX_3$ nanocrystals can also achieve continuous adjustment of the emission wavelength in the full spectral range of visible light by adjusting the ratio of halogen anions at the X site (such as Cl^-/Br^- or Br^-/I^- mixing) [26-30]. Compared with traditional quantum dots, this two-dimensional regulation strategy gives $CsPbX_3$ more excellent color adjustability. However, due to the significant difference in ionic radius between Cl^- (1.81Å) and I^- (2.20Å), their mixed doping will cause lattice distortion, and stable synthesis has not yet been achieved [15].

3.2. Electrical Properties of CsPbX$_3$ Nanocrystals

The electrical properties of $CsPbX_3$ nanocrystals are closely related to the chemical composition of their halogen sites. Due to the differences in ionic radius and electronegativity, different halogen species will directly affect the conductivity and carrier mobility of the material by changing the lattice parameters and energy band structure. Protesescu et al. pointed out that the lattice expansion of

$CsPbX_3$ leads to the increase of Pb-X bond length and the decrease of band gap (Eg: $CsPbCl_3$ > $CsPbBr_3$ > $CsPbI_3$) with the increase of halogen ion radius (Cl^-< Br^-< I^-) [11]. This band gap change significantly affects carrier concentration and transport behavior: narrow band gap $CsPbI_3$ nanocrystals exhibit higher intrinsic conductivity due to smaller exciton binding energy, but their higher defect density may cause non-radiative recombination; the wide band gap $CsPbCl_3$ has a long carrier lifetime due to the strong quantum confinement effect, but the carrier mobility is relatively limited.

In the halogen alloying system, the electronegativity difference of halogen ions can significantly regulate the polarity characteristics of Cs-Pb-X bonds and the spatial distribution of electron clouds. Liu et al. found that the Cs-Pb-Cl system formed by highly electronegative Cl ions has stronger bond polarity, and its enhanced dipole effect effectively promotes the dissociation of photogenerated carriers, so that the open circuit voltage and photoelectric conversion efficiency of the device are systematically improved [31]. This phenomenon reveals that higher electronegative halogens are more likely to induce the separation of electron-hole pairs, which can optimize the carrier transport path and inhibit non-radiative recombination.

PNCs composed of different halogen ions have different carrier mobility. Kovalenko's team [32] confirmed by transient absorption spectroscopy that the carrier mobility of Br/I alloyed nanocrystals can reach the order of 102 $cm^2/(V \cdot s)$, which is close to the level of single crystal silicon. Li Wenzhe's team [33] further solved the problem of $Cs4PbBr_6$ by-products and defects caused by the competitive coordination of Br^-/I^- in PNCs through the introduction of ordered intermediate $PbBrI\text{-}(DMSO)_2$. The photoresponse of ordered $CsPbBr_2I$ with microsecond zoom along the [010] direction was measured, and its carrier mobility was as high as 2574 $cm^2\ V^{-1}s^{-1}$, which was an order of magnitude improvement compared with the non-priority direction.

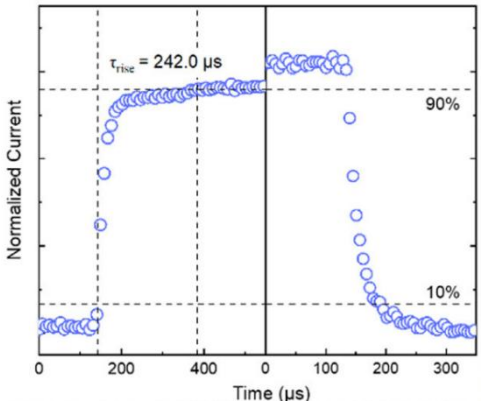

Figure 5. [010] Optical response of microsecond zoom [33].

Halogen vacancies will introduce deep-level trap states, resulting in carrier localization and leakage current phenomena, especially under bias or illumination conditions, aggravating device performance degradation. The dynamic evolution mechanism of halogen component segregation under electric field or illumination is not clear [34], and high concentration doping may cause lattice distortion and enhance carrier scattering [35].

3.3. Stability of $CsPbX_3$ Nanocrystals

The stability study of $CsPbX_3$ nanocrystals is the core issue to promote the practical application of its optoelectronic devices. In recent years, significant progress has been made in the regulation of its environmental stability, chemical stability and photo / thermal stability. The stability of $CsPbX_3$ nanocrystals is mainly affected by halogen components, surface ligand engineering and encapsulation strategies.

The instability of $CsPbX_3$ nanocrystals in water-oxygen environment is due to the high mobility of halogen ions and the presence of surface defect states. $CsPbI_3$ is easily transformed from photoactive α phase to inactive δ phase at room temperature, and the introduction of Br^- can significantly improve the phase stability by reducing the phase transition temperature and lattice strain [36]. The incorporation of Cl^- further enhances the structural rigidity and inhibits the decomposition at high temperature [37]. In addition, photoinduced halogen segregation and thermally induced ion migration are also key factors affecting the stability of PNCs. It was found that the photo-induced polaron in $CsPbI_{1.2}BR_{1.8}$ thin film under continuous illumination induces local strain gradient, which leads to the directional migration of $I^-$and Br^-, forming the separation of iodine-rich phase and bromine-rich phase [38]. Surface modification or encapsulation techniques (such as SiO_2/Al_2SiO_5 composite fibers) can effectively inhibit ion migration and improve environmental stability [36. 37].

4. STUDY ON X-SITE DOPING

4.4. Cl^- Ion Doping

Cl^- doping regulates the optical, electrical properties and stability of $CsPbX_3$ nanocrystals by partially replacing Br^- or I^-. The introduction of Cl^- increases the band gap, resulting in a blue shift of the luminescence peak. The incorporation of 20 % Cl^- in $CsPbBr_3$ can shift the emission wavelength from 515 nm to 480 nm [14].The top of the valence band is dominated by the hybridization of Pb 6s and Cl 3p orbitals, and the bottom of the conduction band is composed of Pb 6p orbitals. This band structure change further optimizes the light absorption and emission properties [39]. The strong coordination between Cl^- and Pb^{2+} can passivate halogen vacancies and inhibit non-radiative recombination, thus prolonging the carrier lifetime. The eutectoid team passivated the SnO_2 electron transport layer through the Cl^- end, which shortened the photocurrent decay lifetime of $CsPbBr_3$ from 2.72 μs to 1.53 μs, and extended the photovoltage decay lifetime to 4.2 μs [40]. In addition, Cl^- doping can optimize the charge transfer path and reduce the interface resistance by adjusting the inclination of perovskite octahedron [41], which is suitable for high-speed photodetectors.

Cl^- doping in $CsPbBr_3$ nanocrystals is mainly achieved by halogen ion exchange or co-synthesis strategy, and the core is the dynamic replacement of Br^- and Cl^-. The Cl^- doping strategy is mainly divided into two categories: Hot injection method: by injecting cesium precursor into the $PbCl_2$ precursor solution to achieve uniform doping. Protesescu et al. synthesized $CsPbCl_3$ nanocrystals by this method for the first time. For every 10 % increase in Cl^- doping, the lattice constant decreases linearly from 5.98 Å (pure Br) to 5.84 Å (x=2.0), and the band gap increases from 2.38 eV to 2.72 eV [11]. The Cl^- doping concentration can be adjusted by optimizing the Cl/Pb ratio, but high temperature can easily lead to the volatilization of halogen, which requires inert atmosphere protection. Room temperature ion exchange method is widely used because of its simple operation. Katelnikovas et al. used TMS-Cl with high reactivity as Cl source to introduce Cl^- into $CsPbBr_3$ lattice at room temperature, and accurately controlled the doping ratio by Cl precursor concentration [42]. After Cl^- doping, the size distribution of PNCs is more uniform, the surface defects are reduced, and the PLQY is as high as 57 %.

The research of Cl^- doping focuses on precise doping control and stability improvement. Zhang proposed a general strategy for non-destructive in-situ halide exchange. Blue perovskites with low trap density and adjustable band gap were obtained by doping long alkyl chain chlorides, and high-efficiency PeLEDs across the blue spectral region were obtained, showing external quantum efficiencies of 23.6 % (sky blue emission at 488 nm), 20.9 % (pure blue emission at 478 nm) and 15.0 % (dark blue emission at 468 nm), respectively [43]. In addition, Feng's team constructed a 2D/3D/2D perovskite double heterojunction in situ to effectively passivate defects in perovskite and reduce ion migration. The inverted double heterojunction PSC shows a high-power conversion efficiency of 24.08 %, and maintains 92 % of the initial value after being stored in N_2 atmosphere

and light for 3000 hours, which provides a new idea for solving the interface defects of perovskite solar cells [44].

Nowadays, Cl^- doping technology has been widely used in optoelectronic devices. Zhao's team proposed a strategy of double surface terminalization of Cl ions and aromatic quaternary ammonium PTA cations to passivate the surface and improve charge separation and transport. The double-passivated $CsPbI_3$ inorganic perovskite cell achieved a photoelectric conversion efficiency of 19.03 % [45]. In terms of LED and display technology, Kumar et al. reported Cl^- doped $CsPbBr_3$ based green LEDs with a maximum brightness of 15,000 cd/m^2 and EQE increased from 6 % to 12 % [46].

4.5. Br^- ion Doping

The doping of Br^- ions (ionic radius: 1.96 Å) can effectively balance the high stability of Cl^- and the narrow band gap characteristics of I^-, thus expanding the application range of materials [47]. Br^- doping can not only realize the continuous adjustment of the emission wavelength from ultraviolet to visible light, but also inhibit non-radiative recombination and ion migration.

By adjusting the ratio of $PbBr_2$ to Cs precursor, the uniform doping of Br^- can be achieved. Protesescu et al. achieved partial substitution of Cl^-/I^- to Br^- by immersing $CsPbCl_3$ or $CsPbI_3$ nanocrystals in a solution containing Br^- precursors, and PLQY was as high as 90 % [11]. Akkerman et al. successfully red-shifted the luminescence peak of $CsPbI_3$ nanocrystals from 680 nm to 520 nm by using room temperature anion exchange method to make the Br^- doping amount up to 70 % [48]. The construction of core-shell quantum dots is an effective strategy to improve the photoelectric properties and stability of perovskite quantum dots. Jin et al. synthesized high-quality core-shell $CsPbBr_3$ @ $CsPb_2Br_5$ perovskite quantum dots by cryoablation strategy, with PLQY up to 95 % and excellent stability [49].

The introduction of Br^- can significantly reduce the band gap of the material. Density functional theory calculations show that the bottom of the conduction band is dominated by the Pb 6p orbital after Br^- doping, and the top of the valence band is formed by the hybridization of Br 4p and Pb 6s orbitals [50, 51]. Yasser et al. developed a Br^- doped $CsPbI_3$ based red LED with a maximum external quantum efficiency (EQE) of 20.3 % and a tunable emission wavelength of 620 - 650 nm, which is superior to pure $CsPbI_3$ devices (EQE ≈ 12 %) [52]. $CsPbBr_3$ nanocrystals exhibit high carrier mobility, and the X-ray detector sensitivity reaches 55684 $\mu C\ Gy_{air}^{-1}\ cm^{-2}$ at an electric field of 5.0 V/mm [53]. This is attributed to the passivation effect of Br^- on surface defects. In addition, Br^- doping can reduce lattice distortion and inhibit the formation of halogen vacancies, and prolong the carrier lifetime.

In recent years, related research has focused on the improvement of stability, multi-functional device integration and environmentally friendly synthesis strategies. In order to achieve high-performance X-ray detection and imaging, Hua et al. developed high-quality shape-controlled $CsPbBr_3$Ar and HBr single crystals in a mixed atmosphere by using an atmosphere-controlled edge-defined thin film feeding growth method [54]. Yang et al. designed and in-situ synthesized multi-site ZnS(AG)-$CsPbBr_3$ heterostructures to tune the bright and fast characteristics of scintillators [55]. In addition, Huang et al. overcame the shortcomings of low solubility of $CsPbBr_3$ perovskite through mechanical grinding-driven engineering, and achieved high-quality $CsPbBr_3$ perovskite films, which provided a new method for the preparation of high-quality perovskite polycrystalline thin film devices [56].

4.6. I^- ion Doping

The ionic radius of I^- is larger than that of Br^-, and its incorporation leads to lattice expansion and band gap reduction, which red-shifts the emission peak position and expands the emission wavelength to the red and near-infrared regions.

Halogen ion exchange method is the mainstream strategy of I^- doping. Nedelcu et al. realized the dynamic replacement of Br^-/I^- by mixing $CsPbBr_3$ nanocrystals with PbI_2 solution [14]. The

introduction of I^- makes the luminescence peak red-shift from 515 nm to 680 nm, and the band gap decreases from 2.38 eV to 1.85 eV. XRD analysis showed that the lattice constant was extended from 5.98 Å (pure Br) to 6.24 Å (x=2.5). In addition, Protesescu et al. synthesized $CsPbBr_{3-x}I_x$ nanocrystals at high temperature by dissolving CsBr, $PbBr_2$ and PbI_2 in octadecene in proportion, which optimized the uniformity of I^- doping [11]. By adjusting the PbI_2 content, the I^- doping ratio can be precisely controlled to achieve continuous regulation of the luminescence color from green to red. The solvent quenching method further optimizes the stability of I^- doping. In 2023, Zhao Yixing 's team used this method to prepare $CsPbX_3$ nanocrystals with uniform size distribution [57]. It exhibits nearly 100 % PLQY and high synthesis yield. Moreover, during the storage process of up to 9 months, there was no obvious agglomeration, and PLQY remained above 90 %.

I^- doping significantly reduces the band gap of $CsPbBr_3$, and the emission peak covers 600 ~ 720 nm. However, high I^- content (x>1.5) leads to lattice distortion, and PLQY decreases from 92 % (pure Br) to 45 % (x=2.0). By introducing thiol ligands to passivate surface defects, Hochan Song et al. restored PLQY to 77 % [58]. In addition, I^- doped PNCs are sensitive to humidity and oxygen. Swarnkar et al. used methyl acetate (MeOAc) to purify perovskite quantum dots, making them stable in cubic phase for several months at room temperature [59].

I^- doped $CsPbBr_3$ PNCs are widely used in red LEDs and solar cells. Chiba et al. prepared red LEDs with emission wavelengths of 653 nm (OAM-I) and 645 nm (An-HI), and the EQE reached 10.7 % [60]. In perovskite solar cells, the I^- doped layer acts as a hole transport layer, and the device efficiency is increased from 18.2 % to 21.5 %. However, the problems of Br/I phase separation and oxidation still need to be solved. Yang et al. proposed a strategy to passivate NCs by potassium bromide [61]. Combined with transmission electron microscopy image analysis, it was confirmed that it could inhibit the halide segregation of NCs, and the stability of PLQY was improved to more than 90 %.

The research of I^- doping focuses on the optimization of red/near-infrared luminescence and the breakthrough of environmental stability. In 2024, Li et al. successfully synthesized strongly constrained $CSPBI_3$ quantum dots with good stability. The introduction of a strongly bound 2-naphthalenesulfonic acid ligand and the use of ammonium hexafluorophosphate to exchange long-chain ligands both improved the charge transport capacity of $CSPBI_3$ quantum dots. Perovskite LEDs emit pure red light at 628 nm, achieving a high external quantum efficiency of 26.04 % [62]. In the same year, Li et al. proposed a universal crystallization path control conversion strategy for the first time, and finally realized the controllable preparation of high-quality ammonium-free $FACsPbI_3$ perovskite films, which completely solved the problem of spatial component heterogeneity of $FACsPbI_3$ perovskite films [63].

5. CONCLUSION

Doping is a means of introducing impurity ions into the target lattice to modify the physical and chemical properties of semiconductors. The X-site ion doping (Cl^-, Br^-, I^- or their combination) of $CsPbX_3$ nanocrystals achieves the optimization of material properties by accurately regulating the lattice structure, electronic energy band and defect state. Halogen doping can not only achieve continuous adjustment of the emission wavelength from ultraviolet to near-infrared (PLQY>90 %), but also significantly enhance the environmental stability and carrier mobility of the material, making it show great potential in the fields of LEDs, solar cells and radiation detection.

However, the current research still faces challenges such as non-uniform doping of halogen ions, phase separation caused by ion segregation under external fields, and reduction of environmental risks of lead. Researchers should analyze the spatial distribution characteristics of doped atoms in nanocrystals by integrating characterization techniques and theoretical simulation methods to achieve atomic-level precision control. On the premise of maintaining high PLQY, effectively reducing the

toxicity of materials, encapsulating nanocrystals with water-resistant matrix materials and systematically exploring the influence mechanism of doping-coating synergistic effect on the stability of materials are the key research directions in the future.

REFERENCES

[1] Fan, Q., Biesold-McGee, G., Pan S., et al. Lead-Free Halide Perovskite Nanocrystals: Crystal Structures, Synthesis, Stabilities, and Optical Properties. Angewandte Chemie. 2020, Vol. 59 (No. 3), p. 1030-1046.

[2] Li, X., Cai, W., Guan, H., et al. Highly stable $CsPbBr_3$ quantum dots by silica-coating and ligand modification for white light-emitting diodes and visible light communication. Chemical Engineering Journal. 2021, Vol. 419, p. 129551.

[3] Li, Y., Dong, J., Chen, T., et al. External photoelectric effect of $CsPbBr_3$ perovskite in X-ray region. Acta Physica Sinica. 2021, Vol. 70 (No. 19), p. 197901.

[4] Tong, G., Chen, T., Li, H., et al. Phase transition induced recrystallization and low surface potential barrier leading to 10.91 %-efficient $CsPbBr_3$ perovskite solar cells. Nano Energy. 2019, Vol. 65 (No.2019), p. 104015.

[5] Wang, S., Bi, C., Yuan, J., et al. Original Core-Shell Structure of Cubic CsPbBr3@Amorphous CsPbBrx Perovskite Quantum Dots with a High Blue Photoluminescence Quantum Yield of over 80 %. ACS Energy Letters. 2018, Vol. 3 (No. 1), p. 245-251.

[6] Kieslich, G., Sun, S., Cheetham, A., et al. An extended Tolerance Factor approach for organic–inorganic perovskites. Chemical Science. 2015, Vol. 6 (No. 6), p. 3430-3433.

[7] Seth, S., Samanta, A. A Facile Methodology for Engineering the Morphology of $CsPbX_3$ Perovskite Nanocrystals under Ambient Condition. Scientific Reports. 2016, Vol. 6 (No. 1), p. 37693.

[8] Udayabhaskararao, T., Kazes, M., Houben, L., et al. Nucleation, Growth, and Structural Transformations of Perovskite Nanocrystals. Chemistry of Materials. 2017, Vol. 29 (No. 3), p. 1302-1308.

[9] Zhang, Z., Zhao, X., Wang, T., et al. Research Progress of Solar Cells Based on Organic–Inorganic Hybrid Perovskites Methylamine Lead Halide. Energy and Environment Focus. 2014, Vol. 3 (No. 4), p. 354-359.

[10] Chen, H., Guo, A., Gu, X., et al. Highly luminescent $CsPbBr_3$ (X=Cl, Br, I) perovskite nanocrystals with tunable photoluminescence properties. Journal of Alloys and Compounds. 2019, Vol. 789 (No.2019), p. 1302-1308.

[11] Protesescu, L., Yakunin, S., Bodnarchuk, M., et al. Nanocrystals of Cesium Lead Halide Perovskites ($CsPbX_3$, X = Cl, Br, and I): Novel Optoelectronic Materials Showing Bright Emission with Wide Color Gamut. Nano Letters. 2015, Vol. 15 (No. 6), p. 3692-3696.

[12] Yang, Z., Wang, M., Qiu, H., et al. Engineering the exciton dissociation in quantum-confined 2D $CsPbBr_3$ nanosheet films. Advanced Functional Materials. 2018, Vol. 28 (No. 14), p. 1705908.

[13] Møller, C., Crystal Structure and Photoconductivity of Cæsium Plumbohalides. Nature. 1958, Vol. 182 (No. 4647), p. 1436.

[14] Nedelcu, G., Protesescu, L., Yakunin, S., et al. Fast Anion-Exchange in Highly Luminescent Nanocrystals of Cesium Lead Halide Perovskites ($CsPbX_3$, X=Cl, Br, I). Nano Letters. 2015, Vol. 15 (No. 8), p. 5635-5640.

[15] Chen, M., Zou, Y., Wu, L., et al. Solvothermal Synthesis of High-Quality All-Inorganic Cesium Lead Halide Perovskite Nanocrystals: From Nanocube to Ultrathin Nanowire. Advanced Functional Materials. 2017, Vol. 27 (No. 23), p. 1701121.

[16] Li, X., Wu, Y., Zhang, S., et al. $CsPbX_3$ quantum dots for lighting and displays: room-temperature synthesis, photoluminescence superiorities, underlying origins and white light-emitting diodes. Advanced Functional Materials. 2016, Vol. 26 (No. 15), p. 2435-2445.

[17] Gao, C., Yu, F., Xiong, Z., et al. 47-Fold EQE improvement in $CsPbBr_3$ perovskite light-emitting diodes via double-additives assistance. Organic Electronics. 2019, Vol. 70 (No. 7), p. 264-271.

[18] Tong, Y., Bladt, E., Aygüler, M., et al. Highly Luminescent Cesium Lead Halide Perovskite Nanocrystals with Tunable Composition and Thickness by Ultrasonication. Angewandte Chemie. 2016, Vol. 55 (No. 44), p. 13887-13892.

[19] Pan, Q., Hu, H., Zou, Y., et al. Microwave-assisted synthesis of high-quality "all-inorganic" $CsPbX_3$ (X = Cl, Br, I) perovskite nanocrystals and their application in light emitting diodes. Journal of Materials Chemistry C. 2017, Vol. 5 (No. 42), p. 10947-10954.

[20] Dissertation: Diwei Zhang. Prepraration, properties and application of perovskite quantum dots and metal-organic famework composites. (PhD dissertation, University of Science and Technology Beijing, China, 2019). p.4.

[21] Liu, H., Guyot-S, P., et al. Magnetoresistance of Manganese-Doped Colloidal Quantum Dot Films. The Journal of Physical Chemistry C. 2015, Vol.119 (No.26), p. 14797-14804.

[22] Li, X., Cao, F., Yu, D., et al. All inorganic halide perovskites nanosystem: synthesis, structural features, optical properties and optoelectronic applications. Small. 2017, Vol. 13 (No. 9), p. 1603996.

[23] Li G., Chen, K., Cui, Y., et al. Stability of Perovskite Light Sources: Status and Challenges. Advanced Optical Materials. 2020, Vol.8 (No. 6), p. 1902012.

[24] Brennan, M. C., Herr, J., Nguyen-Beck, T. S., et al. Origin of the Size-Dependent Stokes Shift in $CsPbBr_3$ Perovskite Nanocrystals. Journal of the American Chemical Society. 2017, Vol. 139 (No. 35), p. 12201-12208.

[25] Ha, S. T., Su, R., Xing, J., et al. Metal halide perovskite nanomaterials: synthesis and applications. Chemical science. 2017, Vol. 8 (No. 4), p. 2522-2536.

[26] Yoon, Y. J., Lee, K. T., Lee, T. K., et al. Reversible, full-color luminescence by post-treatment of perovskite nanocrystals. Joule. 2018, Vol. 2 (No. 10), p. 2105-2116.

[27] Liu, Y., Pan, G., Wang, R., et al. Considerably enhanced exciton emission of CsPbCl 3 perovskite quantum dots by the introduction of potassium and lanthanide ions. Nanoscale. 2018, Vol. 10 (No. 29), p. 14067-14072.

[28] Bi, C., Wang, S., Wen, W., et al. Room-temperature construction of mixed-halide perovskite quantum dots with high photoluminescence quantum yield. The Journal of Physical Chemistry C. 2018, Vol. 122 (No. 9), p. 5151-5160.

[29] Zhou, H., Yuan, S., Wang, X., et al. Vapor growth and tunable lasing of band gap engineered cesium lead halide perovskite micro/nanorods with triangular cross section. ACS nano. 2017, Vol. 11 (No. 2), p. 1189-1195.

[30] Haque, A., Ravi, V, K., Shanker, G, S., et al. Internal heterostructure of anion-exchanged cesium lead halide nanocubes. The Journal of Physical Chemistry C. 2017, Vol. 122 (No. 25), p. 13399-13406.

[31] Liu, M., Johnston, M. B., Snaith, H. J. Efficient planar heterojunction perovskite solar cells by vapour deposition. Nature. 2013, Vol. 501 (No. 7467), p. 395-398.

[32] Kovalenko, M, V., Protesescu, L., Bodnarchuk, M, I. Properties and potential optoelectronic applications of lead halide perovskite nanocrystals. Science. 2017, Vol. 358 (No. 6364), p. 745-750.

[33] Deng, J., Yuan, S., Xiong, H., et al. Br-I ordered $CsPbBr_2I$ perovskite single crystal toward extremely high mobility. Chem. 2023, Vol. 9 (No. 7), p. 1929-1944.

[34] Yu, Y., Liu, X., Zhang, S., et al. Photoinduced phase segregation in wide-bandgap mixed-halide perovskite solar cells. Energy Materials and Devices. 2024, Vol. 2 (No. 2), p. 9370037.

[35] Huang, J., Wang, H., Jia, C., et al. Advances in crystallization regulation and defect suppression strategies for all-inorganic $CsPbX_3$ perovskite solar sells. Progress in Materials Science. 2024, Vol. 141 (No. 3), p. 101223.

[36] Dissertation: Yucong Su: Study on the Stability and Anion Exchange Mechanism of Cesium Lead Halide Perovskites Nanocrystals (Master Thesis, Nanjing University, China 2020). p11.

[37] Shi, J., Wang, Z., Gaponenko, N. V., et al. Stability Enhancement in All-Inorganic Perovskite Light Emitting Diodes via Dual Encapsulation. Small. 2024, Vol. 20 (No. 28), p. 2310478.

[38] Liu, D., Guo, Y., Yin, X., et al. Nucleation Regulation and Anchoring of Halide Ions in All-Inorganic Perovskite Solar Cells Assisted by $CuInSe_2$ Quantum Dots. Advanced Functional Materials. 2023, Vol.33 (No. 7), p. 2210754.

[39] Wei, Z., Wei, Y, H., Xu, S., et al. Electronic structure and effective mass of pristine and Cl-doped $CsPbBr_3$. Chinese Physics B. 2024, Vol. 33 (No. 5), p. 057403.

[40] Zhou, L., Sui, M., Zhang, J., et al. Tailored buried layer passivation toward high-efficiency carbon based all-inorganic $CsPbBr_3$ perovskite solar cell. Chemical Engineering Journal. 2024, Vol. 496, p. 154043.

[41] Milstein, T., Kroupa, D., Gamelin, D., et al. Picosecond Quantum Cutting Generates Photoluminescence Quantum Yields Over 100 % in Ytterbium-Doped $CsPbCl_3$ Nanocrystals. Nano Letters. 2018, Vol. 18 (No. 6), p. 3792-3799.

[42] Katelnikovas, A., Larasati, L., Klimkevicius, V., et al. Anion exchange as an excellent tool to obtain highly efficient blue-emitting all-inorganic perovskite quantum dots. Optical Materials. 2024, Vol. 148, p. 114780.

[43] Zhang, K., Shen, Y., Cao, L., et al. Nondestructive halide exchange via SN_2-like mechanism for efficient blue perovskite light-emitting diodes. Nature Communications. 2024, Vol. 15 (No. 1), p. 10621.

[44] Zhang, H., Bi, Y., Wang, Y., et al. Dual-interface passivation to improve the efficiency and stability of inverted flexible perovskite solar cells by in-situ constructing 2D/3D/2D perovskite double heterojunctions. Journal of Power Sources. 2025, Vol. 629, p. 235973.

[45] Wang, Y., Liu, X., Zhang, T., et al. The Role of Dimethylammonium Iodide in $CsPbI_3$ Perovskite Fabrication: Additive or Dopant. Angewandte Chemie International Edition. 2019, Vol. 58 (No. 46), p. 16691-16696.

[46] Manna, A., Dinda, T., Ghosh, S., et al. $CsPbBr_3$ in the Activation of the C-Br Bond of $CBrX_3$ (X = Cl, Br) under Sunlight. Chemistry of Materials. 2023, Vol. 35 (No. 2), p. 628-637.

[47] Hieulle, J., Wang, X., Stecker, C., et al. Unraveling the impact of halide mixing on perovskite stability. Journal of the American Chemical Society. 2019, Vol. 141 (No. 8), p. 3515-3523.

[48] Akkerman, Q., Innocenzo, V., Accornero, S., et al. Tuning the Optical Properties of Cesium Lead Halide Perovskite Nanocrystals by Anion Exchange Reactions. Journal of the American Chemical Society. 2015, Vol. 137 (No. 32), p. 10276-10281.

[49] Jin, X., Wang, C., Miao, Y., et al. In situ Surface Reconstruction in Pure Water by Ice-Confined Freeze-Thaw Strategy for High-Performance Core-Shell Structural Perovskite Nanocrystals. Advanced Functional Materials. 2024, Vol. 34 (No. 28), p. 2401435.

[50] Maleka, P. M., Dima, R. S., Ntwaeaborwa, O. M., et al. Density functional theory study of Br doped $CsPbI_3$ perovskite for photovoltaic and optoelectronic applications. Physica Scripta. 2023, Vol. 98 (No. 4), p. 045505.

[51] Even, J., Laurent, P., Claudine, K., et al. Solid-State Physics Perspective on Hybrid Perovskite Semiconductors. The journal of physical chemistry, C. Nanomaterials and interfaces. 2015, Vol. 119 (No. 19), p. 10161-10177.

[52] Yasser, H., Park, J., Crawford, M., et al. Ligand-engineered bandgap stability in mixed-halide perovskite LEDs. Nature. 2021, Vol. 591 (No. 7848), p. 72-77.

[53] Pan, W., Yang, B., Niu, G., et al. Hot-pressed $CsPbBr_3$ quasi-monocrystalline film for sensitive direct X-ray detection. Advanced Materials. 2019, Vol. 31 (No. 44), p. 1904405.

[54] Hua, Y., Zhang, G., SUN, X., et al. Suppressed ion migration for high-performance X-ray detectors based on atmosphere-controlled EFG-grown perovskite $CsPbBr_3$ single crystals. Nature photonics. 2024, Vol. 18 (No. 8), p. 870-877.

[55] Yang, Z., Yao, J., Xu, L., et al. Designer bright and fast $CsPbBr_3$ perovskite nanocrystal scintillators for high-speed X-ray imaging. Nature Communications. 2024, Vol. 15 (No. 1), p. 8870.

[56] Huang J, Shuang Z, Zhang X, et al. Mechanical grinding driven engineering enables high-performance $CsPbBr_3$ perovskite photodetectors. IEEE Electron Device Letters. 2024, Vol, 45 (No. 7), p. 1233 - 1236.

[57] Dissertation: Zhao, X. Study on the effect of solvent quenching on the hot injection synthesis and optoelectronic properties of $CsPbX_3$ perovskite nanocrystals. (PhD dissertation, Nanchang University, China, 2023). p.8.

[58] Song, H., Yang, J., Lim, S., et al. On the surface passivating principle of functional thiol towards efficient and stable perovskite nanocrystal solar cells. Chemical Engineering Journal. 2022, Vol. 454 (No. 2), p. 140224.

[59] Swarnkar, A., Ashley, M., Sanehira, E., et al. Quantum dot–induced phase stabilization of α-$CsPbI_3$ perovskite for high-efficiency photovoltaics. Science. 2016, Vol. 354 (No. 6308), p. 92-95.

[60] Chiba, T., Hayashi, Y., Ebe, H., et al. Anion-exchange red perovskite quantum dots with ammonium iodine salts for highly efficient light-emitting devices. Nature photonics. 2018, Vol. 12 (No. 11), p. 681-687.

[61] Yang, J., Yang, S., Yao, J., et al. Potassium Bromide Surface Passivation on $CsPbI_3$-XBrX Nanocrystals for Efficient and Stable Pure Red Perovskite Light-Emitting Diodes. Journal of the American Chemical Society. 2020, Vol. 142 (No. 6), p. 2956-2967.

[62] LI, Y., DENG, M., ZHANG, X., et al. Stable and efficient $CsPbI_3$ quantum-dot light-emitting diodes with strong quantum confinement. Nature Communications. 2024, Vol. 15 (No. 1), p. 5696.

[63] Li, S., Jiang, Y., Xu, J., et al. High-efficiency and thermally stable FA$CsPbI_3$ perovskite photovoltaics. Nature. 2024, Vol. 635 (No. 8037), p. 82-88.